Research Article

Faisal Alsuwayyid, Abdulaziz Alshehri, Khalid Alhelal, Omar Alhuthaili, Mustafa E. Omer, Salam Massadeh, Manal Alaamery, Saleh Alanazi, Faiyaz Shakeel, Majed A. Halwani, Prawez Alam, Alaa Eldeen Yassin*

Near-infrared IR780 dye-loaded poloxamer 407 micelles: Preparation and *in vitro* assessment of anticancer activity

https://doi.org/10.1515/chem-2025-0202 received April 7, 2025; accepted July 25, 2025

Abstract: The aim of this study is to load IR780 into an optimized micellar system that can act as a scaffold, and then test the anticancer activity and micelle stability in various media *in vitro*. Poloxamer 407 was used as the primary polymeric surfactant. Micellar stability tests were carried out in three different media: distilled water, phosphate buffer

* Corresponding author: Alaa Eldeen Yassin, College of Pharmacy, King Saud bin Abdulaziz University for Health Sciences, King Abdullah International Medical Research Center, and King Abdulaziz Medical City, Ministry of National Guard, Health Affairs, Riyadh, Saudi Arabia, e-mail: yassina@ksau-hs.edu.sa

Faisal Alsuwayyid, Abdulaziz Alshehri, Khalid Alhelal, Omar Alhuthaili: College of Pharmacy, King Saud bin Abdulaziz University for Health Sciences, King Abdullah International Medical Research Center, and King Abdulaziz Medical City, Ministry of National Guard, Health Affairs, Riyadh, Saudi Arabia

Mustafa E. Omer: Pharmacy Program, College of Health and Sport Sciences, University of Bahrain, Zallaq, Bahrain

Salam Massadeh, Manal Alaamery: Developmental Medicine Department, King Abdullah International Medical Research Center, King Saud Bin Abdulaziz University for Health Sciences, Riyadh, 11481, Saudi Arabia; Joint Centers of Excellence Program, KACST-BWH/Harvard Center of Excellence for Biomedicine, King Abdulaziz City for Science and Technology (KACST), Riyadh, 11442, Saudi Arabia

Saleh Alanazi: College of Pharmacy, King Saud bin Abdulaziz University for Health Sciences, King Abdullah International Medical Research Center, and King Abdulaziz Medical City, Ministry of National Guard, Health Affairs, Riyadh, Saudi Arabia; Pharmaceutical Care Services, King Abdulaziz Medical City, National Guard Health Affairs (NGHA), Riyadh, 11426, Saudi Arabia

Faiyaz Shakeel: Department of Pharmaceutics, College of Pharmacy, King Saud University, Riyadh, 11451, Saudi Arabia; Jadara University Research Center, Jadara University, Irbid, Jordan

Majed A. Halwani: Nanomedicine Department, King Abdullah International Medical Research Center, King Saud Bin Abdulaziz University for Health Sciences, Riyadh, 11481, Saudi Arabia

Prawez Alam: Department of Pharmacognosy, College of Pharmacy, Prince Sattam bin Abdulaziz University, Al-Kharj, 11942, Saudi Arabia

saline, and Dulbecco's modified Eagle's medium (DMEM). The micelles were evaluated in terms of the micellar size, polydispersity index (PDI), zeta potential, and drug entrapment efficiency (EE). The micelles had an average size of 27.6–354.4 nm. The PDI for all of the micelles ranged between 0.23 and 0.28. The zeta-potential values were extremely low. EE was generally very high, exceeding 90%. Only DMEM showed significant shrinkage in the particle size during the first period of storage, reaching a range of 27.6–37.3 nm, followed by a gradual increase in the micelle size with time. The micelles significantly increased the activity on MCF-7 cells *in vitro*. For more than a month, the micelles exhibited high stability in various media. The prepared system has a high potential for improving anticancer activity against a wide range of cancer cell lines.

Keywords: IR780, poloxamer 407, thin-film hydration, polymeric micelles, MCF-7 cancer cells

1 Introduction

Cancer's worldwide effect as one of the top causes of death remains an enormous healthcare obstacle, with approximately 10 million fatalities and 19.3 million additional newly discovered cancer cases documented as of 2020 [1]. The prevalence of this life-threatening illness has increased dramatically over the last 5 years. Notably, female breast cancer has recently become the leading cause of cancer diagnosis worldwide, surpassing lung cancer incidence [1]. Breast cancer accounted for approximately 11.7% of all cancer incidence in 2020, affecting an estimated 2.3 million people [1]. Breast cancer remains a major cause of cancer-related mortality, despite advances in diagnosis and treatment. It is the fifth largest contributor of cancer fatalities, with a predicted 685,000 deaths [1].

Despite its high toxicity and poor patient quality of life, chemotherapy remains the most commonly used cancer treatment modality [2]. The failure to produce significant anticancer activity capable of reducing the burden of 2 — Faisal Alsuwayyid et al. DE GRUYTER

malignant tumors and the development of intrinsic resistance to cytotoxic drugs are regarded as the primary limitations of cancer chemotherapy [2,3]. Some tumors, such as breast cancer, can develop fundamental and acquired resistance to chemotherapy [4]. These challenges have prompted the scientific community to develop new tools for early detection and more effective treatment. The most common approaches to increasing treatment efficacy while reducing side effects and toxicity are hormonal, immune, monoclonal antibodies, cancer stem cells, photothermal (PTT), and photodynamic therapies [5,6].

PTT is a promising cancer treatment option in which localized heat is generated by exposing a photoabsorbent material to near-infrared radiation (NIR), resulting in hyperthermia within cancerous cells and ablation at 45°C [7,8]. The presence of NIR material capable of generating effective heat and the optimal configuration of the delivery system to maximize its accumulation in cancerous tissues are essential components of success [9,10]. Carbon nanostructures, gold nanoparticles, and various dyes were studied, and they demonstrated high photosensitizing and absorbing properties [11,12]. Photoabsorbent substances that react more efficiently to NIR light with wavelengths of 700–1,000 nm are being investigated as a possible means of treating cancer due to NIR's incredible capacity for penetration in biological tissues, allowing for deep cancer therapy [13].

IR780 iodide, an NIR organic dye, has been shown to benefit both diagnosis and treatment with PTT radiation for various cancer types [14,15]. Its exclusive absorption by organic anion transporter peptides, which are overexpressed in many tumor cells, enables its distribution in cancerous cells, specifically in breast tumors [15,16]. Furthermore, IR780 can produce both concentrated heat and reactive oxygen species when exposed to NIR radiation [15–17]. However, the limited water solubility, short mean residence time, and high toxicity profile indicated by a low maximum tolerance dose of only 1.5 mg/kg in mice are major disadvantages limiting its clinical use [18-20]. Consequently, IR780 iodide is an appealing option for delivery via nanoparticle systems that can improve its therapeutic efficacy and avoid adverse side effects [19,21,22]. Nanoparticulate drug delivery has recently been known as a successful strategy for improving the treatment effectiveness of many anticancer drugs by altering their biopharmaceutical properties as well as their unfavorable and hazardous effects on normal tissues [23,24]. Several types of nanodrug systems, including micelles, liposomes, solid lipid, and polymer-based nanoparticles, have been shown to improve the therapeutic efficacy of many chemotherapy medications [25–28]. As a result, multiple trials have been conducted to overcome IR780's undesirable characteristics, including inclusion into heparin-folic acid, polymeric micelles, and silica nanoparticles [19,29]. Jiang et al. reported that conjugation of IR780 with human serum albumin (nab)

resulted in a 1,000-fold boost in solubility and a 10-fold increase in the highest manageable dose [17]. Nagy-Simon et al. demonstrated that incorporation within gold/pluronic nanoparticles resulted in a significant improvement in anticancer activity when compared to free IR780 [30]. Polymeric micelles received significant attention and introduced a new paradigm of drug delivery systems due to their smaller particle size, simple preparation, sustainability in blood circulation, and the ability to incorporate and protect poorly water-soluble drugs [31-33]. Micelles have proven much success in overcoming poor aqueous solubility and enhancing the pharmacokinetic parameters of many anticancer drugs, including IR780 [31,32]. Furthermore, the ability of polymeric micelles to form monomolecular micelles resulted in greater stability both in vitro and in vivo [33]. A number of recent studies found that incorporating IR780 into polymeric micelles significantly increased its aqueous solubility and tumor uptake while also eliminating any discernible toxicity [34-37]. Taking this into consideration, encasing IR780 iodide in a micellar system may offer another advantage of passive accumulation within tumors via the enhanced permeation and retention (EPR) effect [38]. This effect takes advantage of the tumor vasculature's fundamentally leaky and disordered nature, enabling accumulation of the therapeutic agent to the tumor site [38]. This approach can diminish the toxic effects of IR780 while increasing its cancer cytotoxicity potential. Poloxamer 407 has been studied extensively for drug delivery carriers, including polymeric micelles [39,40]. It has been investigated as an excellent solubilizer, emulsifier, and bioavailability enhancer. Furthermore, its hydrophobic core is relatively bulky, which possibly facilitates high drug solubilization in the micelles [41]. Therefore, poloxamer 407 was selected as the polymeric carrier for the preparation of micelles. Based on all these facts and evidence, the goal of this study is to optimize IR780 iodideloaded Poloxamer 407 micelles as nanocarriers with a high potential for improving anticancer therapeutic effects by maintaining high activity while reducing high toxicity.

2 Materials and methods

2.1 Materials

The dye IR780 iodide, poloxamer 407, fetal bovine serum (FBS), Dulbecco's modified Eagle's medium (DMEM), trizma hydrochloride, ThiolTracker™ violet dye, 3-(4, 5-dimethylthiazolyl-2)-2, 5-diphenyltetrazolium bromide (MTT) reagent, and Annexin V-PI kit were purchased from Sigma Aldrich (St. Louis, MO, USA). Methanol, dimethyl sulfoxide (DMSO), and chloroform solvents of high-performance liquid chromatography grade were obtained locally in Riyadh, Saudi Arabia.

2.2 Preparation of IR780-loaded polymeric micelles

IR780 was successfully encapsulated into poloxamer 407 micelles using the thin-film hydration technique, as previously reported by Chen et al. [42]. Briefly, a true solution of IR780 and poloxamer 407 in chloroform was prepared at IR780/poloxamer 407 ratios of 1:20 and 1:40. Chloroform was evaporated utilizing an IKA rotary-evaporator RV10 V-C system (IKA-Werke GmbH & Co., Staufen, Germany) applying a vacuum pressure of 40 mbar and a rotation speed of 100 rpm at 40 ± 0.5 °C. To avoid any solvent residues, the formed thin film was placed under vacuum for the entire night. To reconstruct the micellar drug dispersion, the dried thin film was hydrated with 10 mL of preheated, de-ionized water at 40°C, and rotated at the same speed for 45 min. After that, the dispersion was incubated using ice for 30 min in an ultrasonic homogenizer at 150 W.

2.3 Determination of particle size, PDI, and zeta potential

A Brookhaven ZetaPALS instrument (Brookhaven Instruments Corporation, Holtsville, NY, USA) was utilized for the determination of particle sizes, PDI, and zeta potentials. The samples from each formulation were first diluted to ~0.1% nanoparticle dispersion before measurements using a 90° detection angle. The mode of Laser Doppler Velocimetry was employed for the determination of zeta potential for the same samples.

2.4 Determination of entrapment efficiency (EE) and drug loading (DL)

Three samples from each formulation were placed in dialysis bags with a 6 kDa cut-off molecular weight. Each bag was firmly tied and placed in 30 mL distilled water (DW) for 1 h. The concentration in the dialysate was determined using a sensitive UV-Vis-NIR spectrophotometry method. The drug EE (%) and DL (%) were determined indirectly using the following equations:

2.5 UV-Vis-NIR spectrophotometry method

A total of 5 mg of IR780 was dissolved in 25 mL of methanol to create a 200 µg/mL working stock solution. By measuring the absorbance at $\lambda = 800$ nm of serially diluted solutions in the range of 5–100 µg/mL, a standard calibration curve was created. For validation, the standard curve was re-developed over the course of three separate days and repeated three times on the same day.

2.6 Transmission electron microscopy (TEM) imaging

Samples were dropped over a 400-mesh copper grid coated with carbon. After being completely dry at room temperature, the images were developed utilizing a JEM-1400 Electron Microscope (JEOL, Tokyo, Japan) applying a 120 kV acceleration voltage.

2.7 Evaluation of the physical stability of micelles

The physical stability of IR780-loaded micelles was evaluated in three different media: DW, phosphate buffer saline (PBS), and DMEM. The samples were kept in a refrigerator (2-8°C) for a maximum of 45 days. The particle size, zeta potential, and PDI were periodically measured at various time intervals.

2.8 Evaluation of in vitro cytotoxicity

The MTT assay was employed to assess the cytotoxicity of IR780-loaded poloxamer 407 micelles in MCF-7 breast cancer cell lines. The cells were allowed to grow at a density of around 3×10^5 cells/mL in a basal medium composed of 1:1 10% FBS:DMEM, containing 1% streptomycin (100 μg/ mL)/penicillin (100 units/mL). Cells were grown in a humidified incubator with 5% CO₂ at 37°C. After reaching

$$EE (\%) = \frac{Wt \text{ of total drug in the formula - Wt of free drug(dialysed)}}{Wt \text{ of total drug}} \times 100, \tag{1}$$

DL (%) =
$$\frac{\text{Wt of total drug in the formula - Wt of free drug(dialysed)}}{\text{(Wt of total drug + Wt of total polymer)}} \times 100.$$
 (2)

confluence, cells were trypsinized (300 µL) and transferred to T-75 flasks. All of the proposed experiments were carried out using cells from passages 3 to 10. MTT assay was performed using 96-well plates to evaluate the cytotoxicity of the two micelle formulations, P1 and P2, using free media as a negative control. The media was replaced after 48 h, regardless of whether the various treatments were present or absent. The cells were cultured as described above, harvested, and trypsinized for counting. In addition, 1×10^4 cells per well in 96-well plates were seeded. Cell viability was assessed after 72 h of incubation with various concentrations of P1 and P2. After incubating cells at specified conditions, 10 µL of MTT (5 mg/mL in PBS) reagent was added to each well and incubated for 30 min until the formation of a purple precipitate. After removing the MTT reagent 100 µL of DMSO was added to each well. The plates were shaken at room temperature for 30 min. Finally, the absorbance at 570 nm was measured using a microplate reader.

3 Results and discussion

3.1 Preparation of IR780-loaded polymeric micelles

The IR780-loaded polymeric micelles were developed using the thin-film hydration method. Two different polymeric micelles, P1 and P2, were prepared. The ratio of the drug to poloxamer 407 was 1:20 and 1:40 in the formulations P1 and P2, respectively. The critical micelle concentration (CMC) of poloxamer 407 was 2.8×10^{-6} M (equivalent to 0.003% w/v)

Table 1: Composition of IR780-loaded polymeric micelle formulations

Code	IR780 (mg)	Poloxamer 407 (mg)	Drug:polymer ratio
Void	_	100	_
P1	5	100	1:20
P2	5	200	1:40

[43]. The concentrations of poloxamer in two different formulations, P1 and P2, were 1.0 and 2.0% w/v, respectively. As a result, the concentrations of poloxamer 407 in both formulations were beyond its CMC level, which would support the formation of micelles. The composition of polymeric micelles is presented in Table 1.

3.2 Particle size, PDI, and zeta potential

The particle size, PDI, and zeta potential of the micellar formulations were measured in three different media: water, PBS, and DMEM. The results of the particle size and PDI are depicted in Figure 1. The average particle size for both formulations in all three media ranged from 27.6 to 354.4 nm (Figure 1a). The average particle sizes of formulations P1 and P2 in water were 354.4 ± 4.2 and 229.4 ± 2.6 nm, respectively. The average particle sizes of formulations P1 and P2 in PBS were found to be 293.1 ± 3.5 and 213.9 \pm 2.8 nm, respectively. In contrast, formulations P1 and P2 in DMEM had average particle sizes of 27.6 \pm 0.9 and 37.3 ± 1.1 nm, respectively. Overall, the average particle size of both formulations was found to be smaller in DMEM than in water or PBS. These results indicated the significant influence of media on the particle size of micellar formulations.

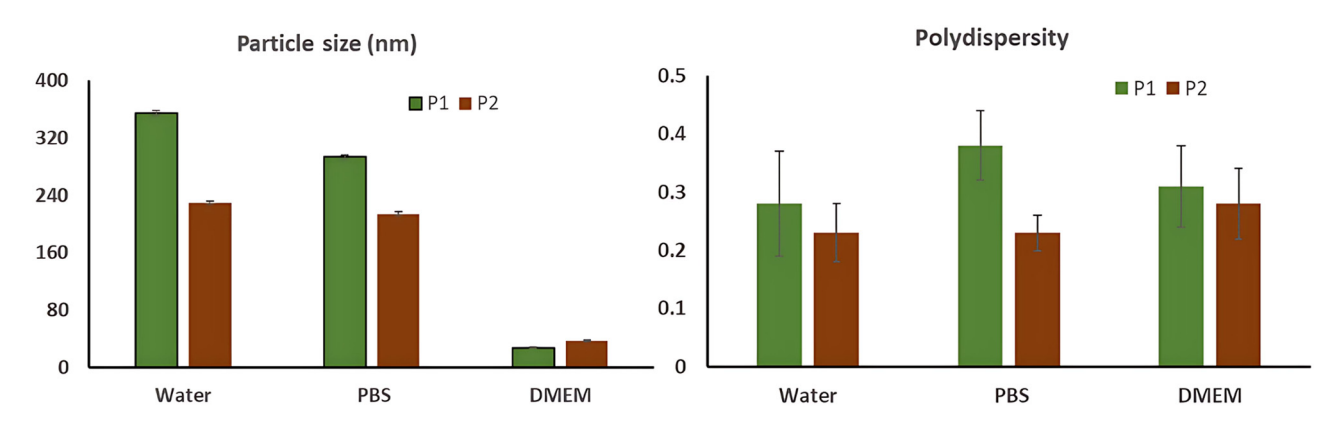


Figure 1: The mean particle sizes and PDIs ± standard deviation for micellar formulations P1 and P2 in three different media: DW, PBS, and DMEM.

The PDIs for both formulations in all three media ranged between 0.23 and 0.38 (Figure 1b). The PDIs for formulations P1 and P2 in water were found to be 0.28 and 0.23, respectively. However, the PDIs of formulations P1 and P2 in PBS were determined as 0.38 and 0.23, respectively. In contrast, formulations P1 and P2 in DMEM had PDIs of 0.31 and 0.28, respectively. Formulation P2 had significantly lower PDIs than P1 in all three investigated media (P < 0.05). Overall, P2 had the lowest PDI in water and PBS (0.23) compared to DMEM. The particle intensity images C, D, and E in Figure 1 clearly show single sharp peaks, indicating a narrow distribution of particle sizes in only one population in the nanorange of 100-200 nm. A threshold value of 0.3 has been embraced in the scientific literature as the upper limit for adequate size uniformity within an individual nanoparticle formulation [44,45]. As a result, the micelle size distribution in both formulations is considered narrow.

The literature emphasizes the importance of particle size in nanoparticulate systems for biological performance [46–49]. This is especially important for polymeric micelles, as demonstrated by Cabral et al. [50], who discovered that micelles smaller than 30 nm can concentrate deeply within poorly permeable tumors. The deeper tumor penetration obtained by smaller nanoparticles did not achieve higher anticancer activity [47].

The zeta-potential values for micellar formulations are listed in Table 2. Zeta potential can be used to evaluate the surface charge density of the micelles. The results indicated that the zeta-potential values of both formulations were low. A zeta-potential value of ±30 mV is widely accepted as a measure of colloidal stability [51]. Other factors influencing micelle stability include the necessary hydrophilic/lipophilic balance, interfacial tension, and adjusting the pH. Rather than having a high charge density, micellar systems are lyophilic (solvent-like) colloids that are stabilized mainly by the formation of a protective solvent sheath [52,53]. It was also reported that hydrophilic micelles with neutral surfaces showed higher ability to diffuse within the mucus layers [54,55].

3.3 Determination of EE and DL

The results of EE and DL are shown in Table 2. Micellar formulations P1 and P2 showed EE% values of 86.3 and 92.5%, respectively. Micellar systems have an advantage in terms of EE. As can be seen in Table 1, formulation P2 with a 40:1 surfactant-to-drug ratio had an average EE% (P < 0.05) of 92.5%, which was significantly higher than that

Table 2: Zeta potential, EE%, and DL% of IR780-loaded polymeric

	Zeta potential (mV)	EE (%)	DL (%)
P1	0.32	86.3	4.1
P2	0.51	92.5	2.3

of formulation P1 with a 20:1 surfactant ratio, which had an average of 86.3%. The higher EE% obtained with the P2 formulation may be attributed to the higher surfactantto-drug ratio. The EE% of a tailored ethosomal formulation was reported to be 80.23% [56], which was significantly lower than the formulation with the greatest optimization, P2 (92.5%) in the present investigation. The DL% values for micellar formulations P1 and P2 were 4.1 and 2.3%, respectively. Both formulations' DL values were significantly lower than their EE values, which could be explained by the presence of a high surfactant concentration in comparison to the drug.

3.4 TEM studies

Figure 2 shows the TEM images for six selected fields of various micellar samples at high magnification power (200,000×). The micelles showed a regular spherical shape. The particles in all images had sizes of around 100 nm or lower, which is significantly lower than that obtained with DLS measurements. The color variation of particle core in images a, b, e, and f clearly demonstrates drug encapsulation in the core of the particles. The morphological characteristics of micelles were identified to be determining factors in their biological behavior, including the residence time, distribution mode within the body, and tissue penetration [57,58]. A couple of studies reported that elongated filomicelles had significantly longer residence time than spherical micelles [59,60].

3.5 Physical stability of micelles

Over a 45-day period, the physical stability of formulations P1 and P2 was assessed in terms of the particle size, PDI, and zeta potential in three different media: DW, PBS, and DMEM. Figure 3 shows the stability results based on the particle size and PDI. From 0 to 45 days of storage, the particle sizes of formulation P1 in water, PBS, and DMEM were measured to be 272.90-354.43, 137.02-331.77, and 27.60-132.70 nm, respectively (Figure 3a). The particle size 6 — Faisal Alsuwayyid et al. DE GRUYTER

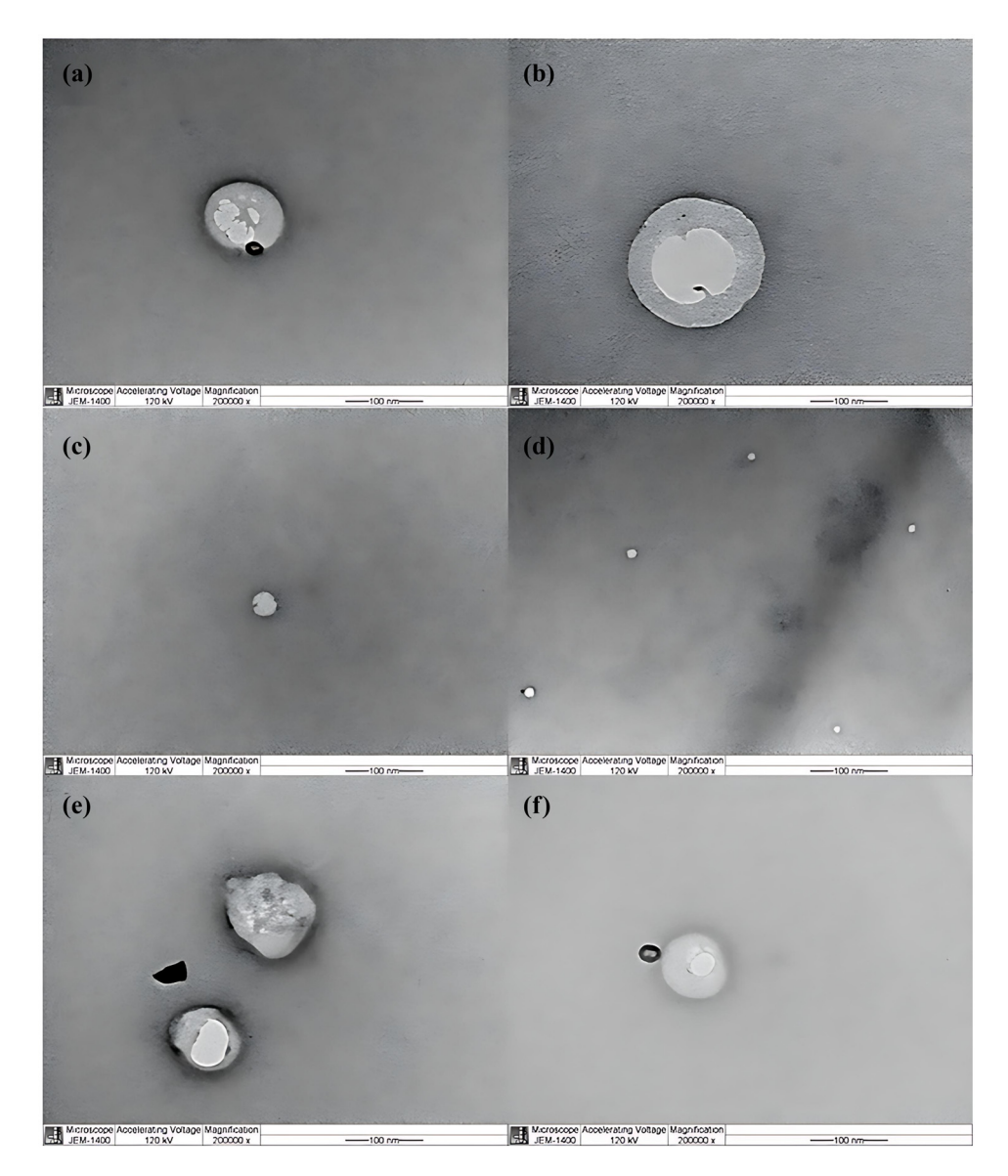


Figure 2: TEM images for an optimized micellar formulation: (a)-(f) different fields at high magnification power (200,000×).

of formulation P1 in water, PBS, and DMEM changed significantly (p < 0.05) from 0 to 45 days of storage. However, from 0 to 45 days of storage, the particle sizes of formulation P2 in water, PBS, and DMEM were measured to be 209.23–234.00, 194.82–356.40, and 209.20–234.00 nm, respectively (Figure 3b). One can conclude that both formulations were reasonably stable in the liquid state, but the size variation was lower in formulation P2 than in P1. It is clear that the particle sizes in DMEM were significantly smaller than in the other two media for both formulations.

The PDIs of formulation P1 in water, PBS, and DMEM were 0.272–0.281, 0.088–0.380, and 0.07–0.362, respectively, from 0 to 45 days of storage (Figure 3c). The PDIs of formulation P1 in water, PBS, and DMEM changed significantly (p < 0.05)

from 0 to 45 days of storage. As a result, formulation P1 was found to be unstable again in water, PBS, and DMEM after 45 days of storage. However, the PDIs of formulation P2 in water, PBS, and DMEM were 0.230–0.284, 0.230–0.322, and 0.056–0.578, respectively, from 0 to 45 days of storage (Figure 3d). Compared to formulation P1, the PDIs of formulation P2 were found to be more consistent, with narrower ranges over 45 days of storage in water and PBS media, whereas they showed greater variation in DMEM. As a result, formulation P2 was found to be generally more stable than formulation P2 in terms of both particle size and size distribution.

The stability of the formulated micelles was investigated in three different media, representing the preparation, biological, and *in vitro* cytotoxicity conditions. The

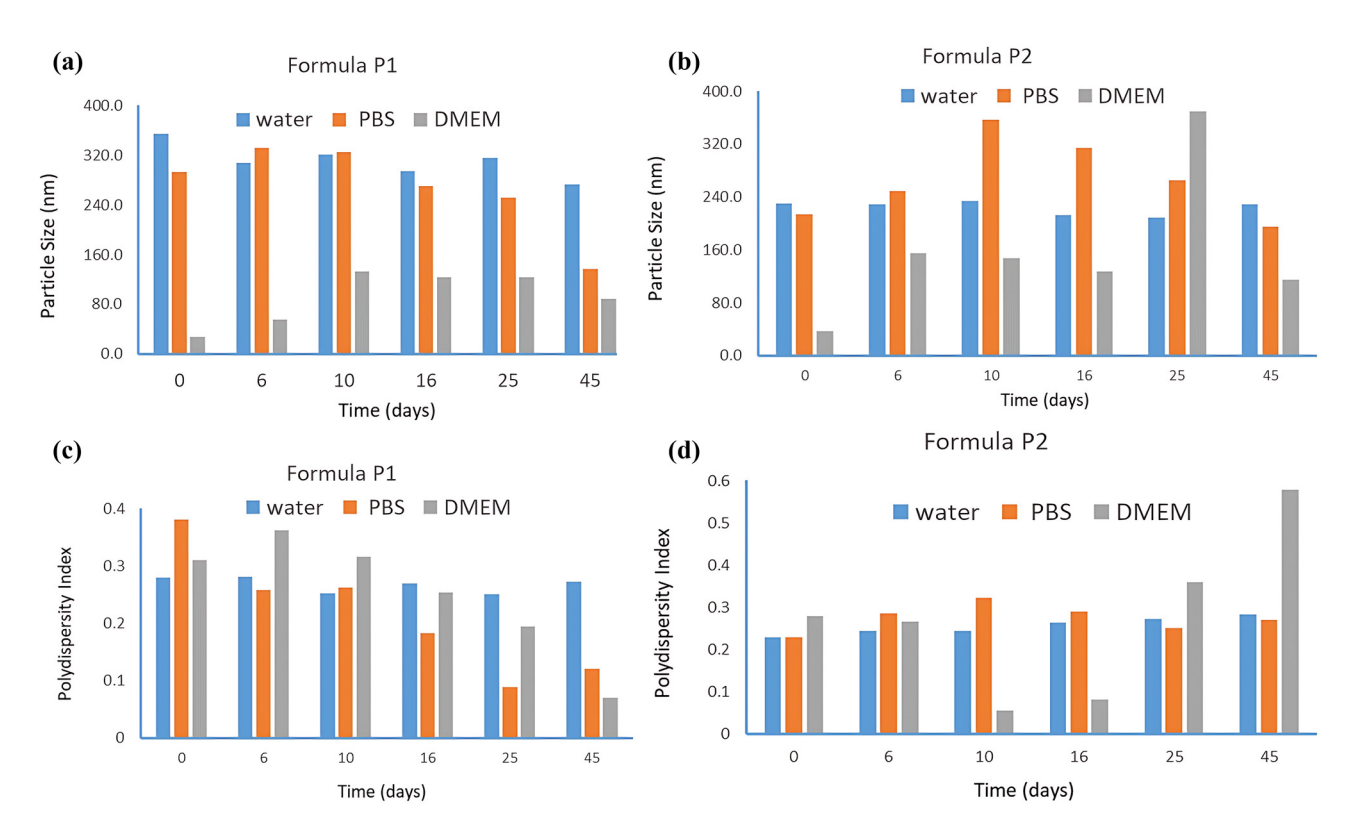


Figure 3: The stability of (a) formulation P1 in terms of particle size, (b) formulation P2 in terms of particle size, (c) formulation P1 in terms of PDI, and (d) formulation P2 in terms of PDI in three different media: DW, PBS, and DMEM over 45 days.

kinetic stability of micelles is a critical parameter that is strongly influenced by changes in the environment surrounding the micelles, such as medium pH, ionic strength, and concentration changes due to dilution [61]. One of the reasons poloxamer 407 was chosen for this study's polymeric micelle formulation is that it can form very stable micelles because it can form a large amount of intermolecular H-bonding, which is thought to be a key physical factor in the stability of polymeric micelles [62]. The observed higher stability of P2 compared to P1 can be attributed to the higher poloxamer 407 ratio, which could

enhance the kinetic stability of micelles [63]. The significantly smaller particle sizes in DMEM in both formulations are expected due to higher ionic strengths caused by the presence of multiple components, which can lead to hypertonic conditions and a negative osmotic effect [61].

The stability results in terms of zeta potential are shown in Figure 4. The zeta potential values of formulation P1 in water, PBS, and DMEM were recorded in the range of -0.28 to 2.15, -11.47 to 2.10, and -0.87 to 7.57 mV, respectively, from 0 to 45 days of storage (Figure 4a). The zeta potential of formulation P1 in water, PBS, and DMEM was

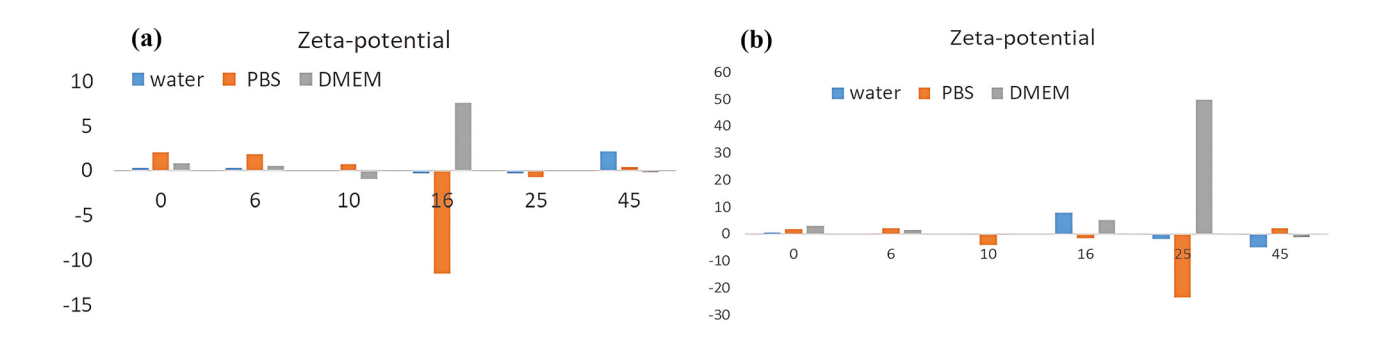


Figure 4: Stability of (a) formulation P1 and (b) formulation P2 in terms of zeta potential in three different media: DW, PBS, and DMEM over 45 days.

8 — Faisal Alsuwayyid et al. DE GRUYTER

Cell viability %

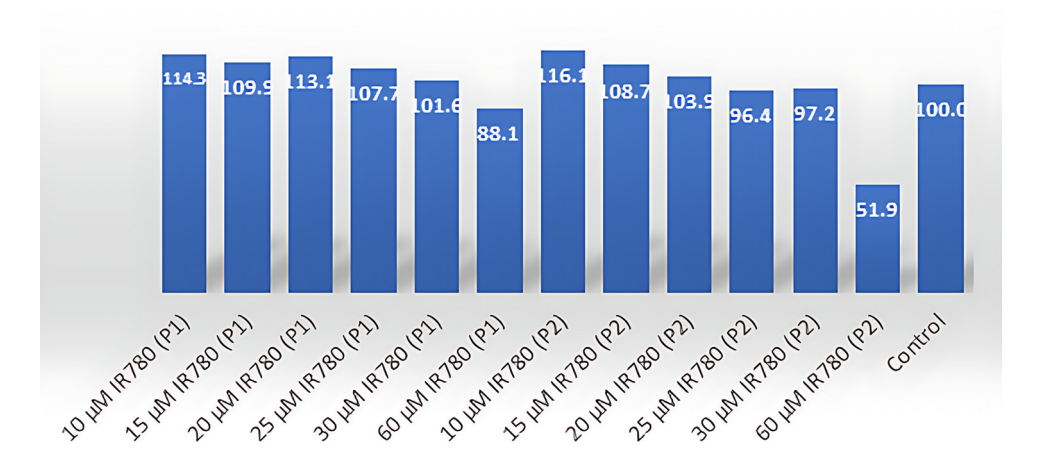


Figure 5: In vitro cytotoxicity results for different concentrations of formulations P1 and P2 in terms of % cell viability.

found to change significantly (p < 0.05) from 0 to 45 days of storage. As a result, formulation P1 was found to be unstable in water, PBS, and DMEM again in terms of zeta potential during 45 days of storage. However, the zeta potential values of formulation P2 in water, PBS, and DMEM were recorded in the range of -0.479 to 7.57, -23.63 to 2.14, and -1.18 to 49.90 mV, respectively, from 0 to 45 days of storage (Figure 4b). The zeta potential values of formulations P1 and P2 in water, PBS, and DMEM were negative initially, but increased significantly after storage and hence became positive after storage. The zeta potential of formulation P2 in water, PBS, and DMEM was also found to change significantly (p < 0.05) from 0 to 45 days of storage. As a result, formulation P2 was also found to be unstable in water, PBS, and DMEM in terms of zeta potential during 45 days of storage. Based on all these results, formulation P2 has been considered more stable than P1.

P2 at concentrations of 10, 15, and 20 µM also showed cell viability of over 100%, indicating no inhibition of MCF-7 breast cancer cells by these concentrations. However, formulation P2 at concentrations of 25, 30, and 60 µM showed cell viabilities of 96.4, 97.2, and 51.9%, respectively, indicating inhibitory activity. Overall, formulation P1 was found to be nontoxic to MCF-7 cancer cells at all studied concentrations. However, formulation P2 was found to be cytotoxic at a concentration of 60 µM. Therefore, formulation P2 can be explored for further preclinical and clinical studies. Although the drug-loaded micelles did not significantly increase cytotoxicity against MCF-7 cell lines, they have the potential to improve the therapeutic efficacy of IR780 by localizing the drug preferentially in tumor tissue for longer periods of time using the EPR phenomenon, resulting in a significant reduction in the aforementioned high drug toxicity.

3.6 In vitro cytotoxicity

The results of *in vitro* cytotoxicity for different concentrations of formulations P1 and P2 are presented in Figure 5. The cell viability of the control was found to be 100%, showing no inhibition of breast cancer MCF-7 cells. Formulation P1 at concentrations of 10, 15, 20, 25, and 30 μM also showed cell viability of over 100%, indicating no inhibition of MCF-7 breast cancer cells. However, formulation P1 at a concentration of 60 μM showed cell viability of 88.1%, indicating slight inhibitory activity. Furthermore, formulation

4 Conclusions

Micelles loaded with IR780 were successfully developed using a highly reproducible thin-film hydration method. The micelles had small particle sizes with a narrow size distribution, high drug EE levels, good integrity, and robustness. The micellar systems had acceptable physicochemical parameters. Formulation P2 had better physicochemical parameters and physical stability in the three different media tested. The cell viability results showed that formulation P2 performed better than formulation P1. The findings of this study suggest that IR780-loaded

micellar systems have a high potential to improve IR780's overall therapeutic performance in the treatment of breast cancer. However, further preclinical and clinical studies are needed to fully understand the potential of the developed micellar systems in the treatment of breast cancer.

Acknowledgments: The authors are thankful to King Abdullah International Medical Research Center (KAIMRC), Ministry of National Guard-Health Affairs, for their generous support via grant no. SP20/501/R.

Funding information: This work was funded by the King Abdullah International Medical Research Center (KAIMRC), Ministry of National Guard-Health Affairs, via grant no. SP20/501/R.

Author contributions: FA: conceptualization, methodology, and investigation; AA: methodology and investigation; KA: methodology and investigation; OA: methodology, investigation; MEO: validation and data curation; SM: formal analysis and data curation; MA: formal analysis and data curation; SA: formal analysis and data curation, writing-review and editing; FS: software, validation, and original draft preparation; MAH: formal analysis and data curation; PA: software, validation, and writing-review and editing; AEY: conceptualization, supervision, project administration, software, resources, funding acquisition, visualization, and writing review and editing.

Conflict of interest: The authors declare no competing financial interests.

Ethical approval: The conducted research is not related to either human or animal use.

Data availability statement: All data generated in this work will be made available upon a reasonable request from the corresponding author.

References

- Sung H, Ferlay J, Siegel RL, Laversanne M, Soerjomataram I, Jemal A, et al. Global cancer statistics 2020: GLOBOCAN estimates of incidence and mortality worldwide for 36 cancers in 185 countries. CA Cancer J Clin. 2021;71(3):209-49.
- [2] Nygren P. What is cancer chemotherapy? Acta Oncol. 2001;40(2-3):166-74.
- Mellor HR, Callaghan R. Resistance to chemotherapy in cancer: A complex and integrated cellular response. Pharmacology. 2008;81(4):275-300.

- Coley HM. Mechanisms and strategies to overcome chemotherapy resistance in metastatic breast cancer. Cancer Treat Rev. 2008;34(4):378-90.
- Debela DT, Muzazu SG, Heraro KD, Ndalama MT, Mesele BW, [5] Haile DC, et al. New approaches and procedures for cancer treatment: Current perspectives. SAGE Open Med. 2021;9:E20503121211034366.
- Charmsaz S, Collins DM, Perry AS, Prencipe M. Novel strategies for cancer treatment: Highlights from the 55th IACR annual conference. Cancers. 2019;11(8):E1125.
- [7] Nomura S, Morimoto Y, Tsujimoto H, Arake M, Harada M, Saitoh D, et al. Highly reliable, targeted photothermal cancer therapy combined with thermal dosimetry using a near-infrared absorbent. Sci Rep. 2020:10(1):E9765.
- Xie X, Shao X, Gao F, Jin H, Zhou J, Du L, et al. Effect of hyperthermia on invasion ability and TGF-B1 expression of breast carcinoma MCF-7 cells. Oncol Rep. 2011;25(6):1573-9.
- Bagley AF, Hill S, Rogers GS, Bhatia SN. Plasmonic photothermal heating of intraperitoneal tumors through the use of an implanted near-infrared source. ACS Nano. 2013;7(9):8089-97.
- Chen F, Cai W. Nanomedicine for targeted photothermal cancer therapy: Where are we now? Nanomedicine. 2015;10(1):1-3.
- Jaque D, Martínez Maestro L, Del Rosal B, Haro-Gonzalez P, [11] Benayas A, Plaza JL, et al. Nanoparticles for photothermal therapies. Nanoscale. 2014;6(16):9494-530.
- Chen WR, Adams RL, Carubelli R, Nordquist RE. Laserphotosensitizer assisted immunotherapy: A novel modality for cancer treatment. Cancer Lett. 1997;115(1):25-30.
- Dong H, Du SR, Zheng XY, Lyu GM, Sun LD, Li LD, et al. Lanthanide [13] nanoparticles: From design toward bioimaging and therapy. Chem Rev. 2015;115(19):10725-815.
- Yuan A, Wu J, Tang X, Zhao L, Xu F, Hu Y. Application of nearinfrared dyes for tumor imaging, photothermal, and photodynamic therapies. J Pharm Sci. 2013;102(1):6-28.
- [15] Luo S, Zhang E, Su Y, Cheng T, Shi C. A review of NIR dyes in cancer targeting and imaging. Biomaterials. 2011;32(29):7127-38.
- [16] Tan X, Luo S, Wang D, Su Y, Cheng T, Shi CA. NIR heptamethine dye with intrinsic cancer targeting, imaging and photosensitizing properties. Biomaterials. 2012;33(7):2230-9.
- [17] Jiang C, Cheng H, Yuan A, Tang X, Wu J, Hu Y. Hydrophobic IR780 encapsulated in biodegradable human serum albumin nanoparticles for photothermal and photodynamic therapy. Acta Biomater. 2015;14:61-9.
- [18] Yue C, Liu P, Zheng M, Zhao P, Wang Y, Ma Y, et al. IR-780 dye loaded tumor targeting theranostic nanoparticles for NIR imaging and photothermal therapy. Biomaterials. 2013;34(28):6853-61.
- Peng CL, Shih YH, Lee PC, Hsieh TMH, Luo TY, Shieh MJ. Multimodal image-guided photothermal therapy mediated by 188Re-labeled micelles containing a cyanine-type photosensitizer. ACS Nano. 2011;5(7):5594-607.
- Wang L, Niu C. IR780-based nanomaterials for cancer imaging and therapy. J Mater Chem B. 2021;9(20):4079-97.
- Zhang C, Wang S, Xiao J, Tan X, Zhu Y, Su Y, et al. Sentinel lymph [21] node mapping by a near-infrared fluorescent heptamethine dye. Biomaterials. 2010;31(7):1911-7.
- [22] Huang B, Wang L, Tang K, Chen S, Su Y, Liao H, et al. IR780 based sonotherapeutic nanoparticles to combat multidrug-resistant bacterial infections. Front Chem. 2022;10(24):E840598.
- [23] Farokhzad OC, Langer R. Impact of nanotechnology on drug delivery. ACS Nano. 2009;3(1):16-20.

- [24] Youan BBC. Impact of nanoscience and nanotechnology on controlled drug delivery. Nanomedicine. 2008;3(4):401–6.
- [25] Soppimath KS, Aminabhavi TM, Kulkarni AR, Rudzinski WE. Biodegradable polymeric nanoparticles as drug delivery devices. J Controlled Release. 2001;70(1–2):1–20.
- [26] Yassin AEB, Albekairy A, Alkatheri A, Sharma RK. Anticancer-loaded solid lipid nanoparticles: high potential advancement in chemotherapy. Dig J Nanomater Biostr. 2013;8(2):905–16.
- [27] Jones MC, Leroux JC. Polymeric micelles-A new generation of colloidal drug carriers. Eur J Pharm Biopharm. 1999;48(2):101–11.
- [28] Yassin AEB, Anwer MK, Mowafy HA, El-Bagory IM, Bayomi MA, Alsarra IA. Optimization of 5-fluorouracil solid-lipid nanoparticles: A preliminary study to treat colon cancer. Int J Med Sci. 2010;7(6):398–408.
- [29] Singh AK, Hahn MA, Gutwein LG, Rule MC, Knapik JA, Moudgil BM, et al. Multi-dye theranostic nanoparticle platform for bioimaging and cancer therapy. Int J Nanomed. 2012;7:2739–50.
- [30] Nagy-Simon T, Potara M, Craciun AM, Licarete E, Astilean S. IR780dye loaded gold nanoparticles as new near infrared activatable nanotheranostic agents for simultaneous photodynamic and photothermal therapy and intracellular tracking by surface enhanced resonant Raman scattering imaging. J Colloid Interface Sci. 2018;517:239–50.
- [31] Rangel-Yagui CO, Pessoa Jr A, Tavares LC. Micellar solubilization of drugs. J Pharm Pharm Sci. 2005;8(2):147–63.
- [32] Mall S, Buckton G, Rawlins DA. Dissolution behaviour of sulphonamides into sodium dodecyl sulfate micelles: A thermodynamic approach. J Pharm Sci. 1996;85(1):75–8.
- [33] FitzGerald PA, Chatjaroenporn K, Warr GG. Structure and composition of mixed micelles of polymerized and monomeric surfactants. | Colloid Interface Sci. 2015;449:377–82.
- [34] He B, Hu HY, Tan T, Wang H, Sun KX, Li YP, et al. IR-780-loaded polymeric micelles enhance the efficacy of photothermal therapy in treating breast cancer lymphatic metastasis in mice. Acta Pharmacol Sin. 2018;39(1):132–9.
- [35] Yuan A, Qiu X, Tang X, Liu W, Wu J, Hu Y. Self-assembled PEG-IR-780-C13 micelle as a targeting, safe and highly-effective photothermal agent for in vivo imaging and cancer therapy. Biomaterials. 2015;51:184–93.
- [36] Deng L, Guo W, Li G, Hu Y, Zhang LM. Hydrophobic IR780 loaded sericin nanomicelles for phototherapy with enhanced antitumor efficiency. Int J Pharm. 2019;566:549–6.
- [37] Chen Y, Li Z, Wang H, Wang Y, Han H, Jin Q, et al. IR-780 loaded phospholipid mimicking homopolymeric micelles for near-IR imaging and photothermal therapy of pancreatic cancer. ACS Appl Mater Interfaces. 2016;8(11):6852–8.
- [38] Maeda H, Wu J, Sawa T, Matsumura Y, Hori K. Tumor vascular permeability and the EPR effect in macromolecular therapeutics: A review. J Controlled Rel. 2000;65(1–2):271–84.
- [39] Bodratti AM, Alexandridis P. Formulation of ploxamers for drug delivery. J Funct Biomater. 2018;9(1):E11.
- [40] Sedlarikova J, Janalikova M, Egner P, Pleva P. Poloxamer-based mixed micelles loaded with thymol or eugenol for topical applications. ACS Omega. 2024;9(22):23209–19.
- [41] Jindal N, Mehta SK. Nevirapine loaded poloxamer 407/pluronic P123 mixed micelles: Optimization of formulation and in vitro evaluation. Coll Surf B. 2015;129:100–6.
- [42] Chen Y, Zhang W, Gu J, Ren Q, Fan Z, Zhong W, et al. Enhanced antitumor efficacy by methotrexate conjugated Pluronic mixed

- micelles against KBv multidrug resistant cancer. Int J Pharm. 2013;452(1–2):421–33.
- [43] Suksiriworapong J, Rungvimolsin T, A-gomol A, Junyaprasert VB, Chantasart D. Development and characterization of lyophilized diazepam-loaded polymeric micelles. AAPS PharmSciTech. 2014;15(1):52–64.
- [44] Kashanian S, Azandaryani AH, Derakhshandeh K. New surface-modified solid lipid nanoparticles using N-glutaryl phosphatidylethanolamine as the outer shell. Int J Nanomed. 2011;6:2393–401.
- [45] Yassin AEB, Massadeh S, Alshwaimi AA, Kittaneh RH, Omer ME, Ahmad D, et al. Tween 80-based self-assembled mixed micelles boost valsartan transdermal delivery. Pharmaceuticals. 2024:17(1):E19.
- [46] Yue J, Liu S, Xie Z, Xing Y, Jing X. Size-dependent biodistribution and antitumor efficacy of polymer micelle drug delivery systems.
 J Mater Chem B. 2013;1(34):4273–80.
- [47] Wang J, Mao W, Lock LL, Tang J, Sui M, Sun W, et al. The role of micelle size in tumor accumulation, penetration, and treatment. ACS Nano. 2015;9(7):7195–206.
- [48] Hoshyar N, Gray S, Han H, Bao G. The effect of nanoparticle size on in vivo pharmacokinetics and cellular interaction. Nanomedicine. 2016;11(6):673–92.
- [49] Sun Q, Ojha T, Kiessling F, Lammers T, Shi Y. Enhancing tumor penetration of nanomedicines. Biomacromolecules. 2017;18(5):1449–59.
- [50] Cabral H, Matsumoto Y, Mizuno K, Chen Q, Murakami M, Kimura M, et al. Accumulation of sub-100 nm polymeric micelles in poorly permeable tumours depends on size. Nat Nanotechnol. 2011;6(12):815–23.
- [51] Thatipamula R, Palem C, Gannu R, Mudragada S, Yamsani M. Formulation and in vitro characterization of domperidone loaded solid lipid nanoparticles and nanostructured lipid carriers. Daru J Pharm Sci. 2011;19(1):23–32.
- [52] Verwey EJW. Theory of the stability of lyophobic colloids. J Phys Colloid Chem. 1947;51(3):631–6.
- [53] Ding B, Ahmadi SH, Babak P, Bryant SL, Kantzas A. On the stability of pickering and classical nanoemulsions: Theory and experiments. Langmuir. 2023;39(20):6975–91.
- [54] Bandi SP, Kumbhar YS, Venuganti WK. Effect of particle size and surface charge of nanoparticles in penetration through intestinal mucus barrier. J Nanopart Res. 2020;22(3):E62.
- [55] Taipaleenmaki E, Brodszkij E, Stadler B. Mucopenetrating zwitterionic micelles. ChemNanoMat. 2020;6(5):744–50.
- [56] Bhosale SS, Avachat AM. Design and development of ethosomal transdermal drug delivery system of valsartan with preclinical assessment in Wistar albino rats. J Liposome Res. 2013;23(2):119–25.
- [57] Kuntsche J, Horst JC, Bunjes H. Cryogenic transmission electron microscopy (cryo-TEM) for studying the morphology of colloidal drug delivery systems. Int J Pharm. 2011;417:120–37.
- [58] Truong NP, Whittaker MR, Mak CW, Davis TP. The importance of nanoparticle shape in cancer drug delivery. Expert Opin Drug Delivery. 2015;12(1–2):129–42.
- [59] Christian DA, Cai S, Garbuzenko O, Harada T, Zajac AL, Minko T, et al. Flexible filaments for in vivo imaging and delivery: persistent circulation of filomicelles opens the dosage window for sustained tumor shrinkage. Mol Pharm. 2009;6(5):1343–52.

- [60] Sancho Oltra N, Swift J, Mahmud A, Rajagopal K, Loverde SM, Discher DE. Filomicelles in nanomedicine – from flexible, fragmentable, and ligand-targetable drug carrier designs to combination therapy for brain tumors. J Mater Chem B. 2013;1(39):E5177.
- [61] Owen SC, Chan DPY, Shoichet MS. Polymeric micelle stability. Nano Today. 2012;7(1):53–65.
- [62] Shi Y, Lammers T, Storm G, Hennink WE. Physico-chemical strategies to enhance stability and drug retention of polymeric micelles for tumor-targeted drug delivery. Macromol Biosci. 2017;17(1):E1600160.
- [63] Haliloglu T, Bahar I, Erman B, Mattice WL. Mechanisms of the exchange of diblock copolymers between micelles at dynamic equilibrium. Macromolecules. 1996;29(10):4764–71.